TUTORIAL/ARTICLE DIDACTIQUE

Canonical perturbation theory for highly excited dynamics

Marc Joyeux and Dominique Sugny

Abstract: This article proposes an unified presentation of recent results dealing with canonical perturbation theory (also called the contact transformation method in the quantum mechanical context), which shows how the theory is best handled for investigating the highly excited dynamics of small molecules. The following systems are successively addressed: (*i*) semi-rigid molecules (one electronic surface, one minimum), (*ii*) floppy molecules (one electronic surface, several minima), and (*iii*) non-Born–Oppenheimer dynamics (several interacting electronic surfaces). The perturbative Hamiltonians obtained from the proposed procedures are checked against exact calculations performed on ab initio surfaces (HCP and HCN) and model Hamiltonians.

PACS No.: 31.15Md

Résumé : Cet article propose une présentation unifiée de résultats récents portant sur la théorie des perturbations canoniques (aussi appelée la méthode des transformations de contact en mécanique quantique), qui ont montré comment utiliser au mieux les divers degrés de liberté de la théorie pour étudier la dynamique de molécules très excitées. On s'intéresse successivement aux systèmes suivants : (*i*) les molécules semi-rigides (une seule surface électronique, un seul minimum), (*ii*) les molécules souples (une seule surface électronique, plusieurs minima) et (*iii*) la dynamique non-Born–Oppenheimer (plusieurs surfaces électroniques couplées). Les Hamiltoniens perturbatifs que l'on obtient par les procédures décrites dans cet article sont comparés à des calculs quantiques exacts portant sur des surfaces d'énergie potentielle ab initio (pour HCP et HCN) et des Hamiltoniens modèles.

1. Introduction

Physicists were not able to compute the exact spectra of all but the most simple systems until recently, because the exact quantum energy levels and wave functions are obtained from the diagonalization of (usually) large Hamiltonian matrices. Fortunately, theoretical tools were developed very early, and they allow a precise determination of quantum spectra at low energies without having recourse to direct

Received 16 April 2002. Accepted 12 June 2002. Published on the NRC Research Press Web site at http://cjp.nrc.ca/ on 10 December 2002.

M. Joyeux[1] and D. Sugny. Laboratoire de Spectrométrie Physique (CNRS UMR 5588), Université Joseph Fourier – Grenoble I, B.P. 87, 38402 St. Martin d'Hères, France.

[1]Corresponding author (e-mail: Marc.JOYEUX@ujf-grenoble.fr).

 DOI: 10.1139/P02-075

diagonalization. These tools are known as perturbation methods. Their role in the development of quantum mechanics was emphasized by Kemble: "In quantum mechanics …perturbation methods are of fundamental importance due to the fact that so few problems can be rigorously solved by direct attack" [1]. The oldest perturbation theory is known as the Rayleigh–Schrödinger's method [2]. It was, however, quickly recognized that this method requires "tedious summations over a large number of intermediate states and that there is a large degree of cancellation in the final algebraic reductions" [3]. Beyond first-order theory, another method, known as canonical perturbation theory (CPT) (or the contact transformation method), is better suited for the purpose of practical calculations. CPT was first introduced in physics by Van Vleck to investigate spin multiplets and σ-type doubling in the spectra of diatomic molecules [4] and was applied 10 years later by Wilson and Howard [5], Shaffer and Nielsen [6], and Shaffer et al. [7] to the vibration–rotation problem in polyatomic molecules. The 1951 review paper by Nielsen [8] can be considered as a pillar of high-resolution spectroscopy.

Modern computers and algorithms make it possible to calculate, variationally, the whole rovibrational spectrum of triatomic molecules from the ground state up to the dissociation threshold and more (several hundreds of converged states) while, roughly, the first 100 states of tetratomic molecules and the first 10 states of pentatomic molecules are becoming gradually amenable to calculations. This, however, does not diminish the practical importance of CPT, for two principal reasons. First, variational calculations are still not routine and remain reserved for specialists. In contrast, the perturbative computation of the spectrum of molecules with up to five atoms requires little programming effort and CPU time. This point of view was recently investigated in detail by Sibert and co-workers [9–12]. Moreover, the perturbative Hamiltonian obtained from CPT is expressed in terms of as complete as possible a set of good quantum numbers, so that this Hamiltonian is a very convenient starting point for understanding the dynamics of a molecule, especially when subjected to a semiclassical analysis (see, for example, refs. 13 and 14; for recent reviews see refs. 15 and 16). The main constraint to a still more widespread use of CPT in the domain of molecular physics is probably the long-standing idea that CPT is suitable for studying only the low-lying states of an uncoupled electronic surface of a semi-rigid molecule. The aim of this article is to report on some recent advances that show that this is certainly not the case. More precisely, it will be shown how CPT must be handled to adapt to (*i*) highly excited vibrational states of molecules with a single equilibrium position (semi-rigid molecules), (*ii*) highly excited vibrational states of molecules with several equilibrium positions (floppy molecules), and (*iii*) highly excited vibrational states of molecules with several coupled electronic surfaces.

Part of the results presented below have already been published elsewhere [13,14,17–20]. However, a classical Birkhoff–Gustavson's perturbation method [21–24] was used in refs. 13, 14, 17, and 18 to study the highly excited states of semi-rigid and floppy molecules, respectively, while the study of coupled electronic surfaces in refs. 19 and 20 is necessarily based on the quantum mechanical Van Vleck perturbation method [1,4,9,25–29]. As Birkhoff–Gustavson's and Van Vleck's methods are conceptually rather different (although they lead to comparable results), all calculations were performed again according to Van Vleck's formalism for the sake of a clearer presentation and to emphasize more firmly the important points of the procedure. Moreover, we have just derived a more elegant and powerful method for studying floppy molecules than the one presented in refs. 14 and 18, while the method for studying coupled electronic surfaces presented in refs. 19 and 20 could be simplified without loss of precision. These new procedures are presented in Sects. 4 and 5 as they were not given in refs. 13, 14, 17, and 18.

The remainder of this article is organized as follows. The principles of Van Vleck's CPT are recalled in Sect. 2. How this theory is best handled for studying the highly excited vibrational dynamics of various systems is the subject of the next three sections: semi-rigid molecules are discussed in Sect. 3, floppy molecules in Sect. 4, and molecules with interacting electronic surfaces in Sect. 5. Finally, some points that deserve further attention are briefly mentioned in Sect. 6.

2. The principles of Van Vleck's perturbation theory

Canonical perturbation methods rely on the fact that, given a unitary transformation U, a Hamiltonian H and its transform K

$$K = UHU^{-1} \tag{2.1}$$

have the same spectrum. Note, however, that the wave functions ψ of H and ϕ of K are obviously not identical, but are instead related through

$$\phi = U\psi \tag{2.2}$$

CPT consists of a series of unitary transformations like (2.1) that are aimed at finding the best set of conjugate coordinates (i.e., position coordinates and conjugate momenta) to express the Hamiltonian. Note that these transformations usually involve the mixing of coordinates and momenta. The "best" set of conjugate coordinates depends largely on the context. For people like us who are interested in dynamical studies and particularly in semiclassical analyses [13–16], the best set of conjugate coordinates is the one for which the non-integrable part of the final Hamiltonian is as small as possible; this part is usually discarded for the purpose of semiclassical studies. Roughly speaking, the best set of conjugate coordinates is approximate actions and angles of the initial Hamiltonian. People like Sibert and co-workers, who are more concerned with the calculation of spectra and eigenvector-related properties [9–12,28], are usually less demanding; their goal is to find a set of conjugate coordinates for which the Hamiltonian matrix factorizes into blocks of easily diagonalizable size, while the terms coupling the blocks should become as small as possible before they are neglected. As will be described in some detail in the next sections, the power of CPT lies in the existence of simple algorithms for transforming gradually from the initial set of conjugate coordinates to the final one.

Lengyel suggested to Kemble [1] that the transformation U should be given the form

$$U = \exp(iS) \tag{2.3}$$

where S is Hermitian, and this form has been widely adopted since then. We instead prefer to use a slightly different form for U, namely,

$$U = \exp(S) \tag{2.4}$$

where S is anti-Hermitian, because (2.4) leads to real coefficients for all the computed series (see below), while (2.3) leads to purely imaginary ones. Let us recall that the exponential of an operator is defined as

$$\exp(S) = \sum_{k=0}^{\infty} \frac{1}{k!} S^k = 1 + S + \frac{S^2}{2} + \frac{S^3}{6} + \ldots \tag{2.5}$$

The reason for writing U in the form of (2.4) is twofold. First, the inverse transformation is just $U^{-1} = \exp(-S)$. Moreover, if S is small enough, as must be the case for every perturbation procedure, then, according to (2.5), the transformation consists of identity plus corrections, the importance of which decreases with power. The perturbation procedure, therefore, consists in finding a series of anti-Hermitian operators $S^{(k)}$, such that

$$\begin{aligned} H^{(1)} &= \exp(S^{(1)})\ H^{(0)}\ \exp(-S^{(1)}) \\ H^{(2)} &= \exp(S^{(2)})\ H^{(1)}\ \exp(-S^{(2)}) \\ &\vdots \\ H^{(s)} &= \exp(S^{(s)})\ H^{(s-1)}\ \exp(-S^{(s)}) \\ &\vdots \end{aligned} \tag{2.6}$$

where $H^{(0)} = H$ is the initial Hamiltonian and $s = 1, 2, \ldots$ is the perturbation order. Simple algebra shows that the transformation at any order s can be rewritten in the most useful form

$$H^{(s)} = H^{(s-1)} + [S^{(s)}, H^{(s-1)}] + \frac{1}{2!}[S^{(s)}, [S^{(s)}, H^{(s-1)}]] + \frac{1}{3!}[S^{(s)}, [S^{(s)}, [S^{(s)}, H^{(s-1)}]]] + \ldots \quad (2.7)$$

where square brackets denote the commutator of two operators, i.e., $[A, B] = AB - BA$. Equation (2.7) is known as the Campbell–Hausdorf formula. At this point, it should be clear that high-order perturbative calculations can only be performed for relatively simple expressions of the initial Hamiltonian, because the evaluation of the nested commutators in (2.7) rapidly becomes cumbersome for too-complex expressions. This is why the first step of most of the perturbative calculations dealing with semi-rigid molecules usually consists of a Taylor expansion of the exact Hamiltonian in the neighborhood of the equilibrium position. Nonetheless, there is some freedom in the form of expansion that is chosen as input Hamiltonian in perturbative calculations. Trigonometric expansions are, for example, also amenable to perturbative calculations [14,18,30–35]. It will be shown in Sect. 4 that mixed polynomial–trigonometric expansions are best suited for studying the vibrational dynamics of floppy molecules. A further remark concerns kinetic energy. Indeed, it is well known that the exact quantum expression for kinetic energy contains extra-potential terms compared with the symmetrized classical expression [36]. These terms might be rather lengthy to calculate, while their influence on eigenvalues and eigenvectors is expected to remain small, usually less than 1 cm^{-1} [37]. Not to let perturbative calculations become unnecessarily complex, we chose to neglect these extra-potential terms systematically, that is, to simply expand and symmetrize the classical expression for kinetic energy.

The principal flexibility of CPT consists of the choice of the operator $S^{(s)}$ at each order s of the perturbation procedure. Although not mandatory [20], this choice is usually guided by the introduction of an artificial book-keeping parameter λ, the "meaning of which is to show the order of magnitude of the product of two or more operators having various orders of magnitudes and group the products accordingly" [29] (λ is set to 1 at the end of the calculations). More precisely, each interpolation Hamiltonian $H^{(s)}$ is expanded in the form

$$H^{(s)} = \sum_k \lambda^k H^{(s,k)} \quad (2.8)$$

while the transformation at order s gives

$$H^{(s)} = \exp\left(\lambda^s S^{(s)}\right) H^{(s-1)} \exp(-\lambda^s S^{(s)}) \quad (2.9)$$

After expansion according to Campbell–Hausdorf's formula, one gets, by equating the powers of λ

$$\begin{aligned} &\text{if} \quad k < s, \quad H^{(s,k)} = H^{(s-1,k)} \\ &\text{if} \quad k = s, \quad H^{(s,s)} = H^{(s-1,s)} + \left[S^{(s)}, H^{(0,0)}\right] \\ &\text{if} \quad k > s, \quad H^{(s,k)} = H^{(s-1,k)} + \sum_m \frac{1}{n!}[\underbrace{S^{(s)}, \ \ldots [S^{(s)}}_{n \text{ times}}, H^{(s-1,m)}] \ldots] \end{aligned} \quad (2.10)$$

(in the last equation, the summation runs over all the integers m, for which there exists another integer n larger than or equal to 1, such that $m + ns = k$). The first equation in (2.10) shows that the transformation at order s does not affect the terms of order smaller than s. The second equation in (2.10) is used to determine the operator $S^{(s)}$, by requiring that $H^{(s,s)}$ contains only the physically important terms

of $H^{(s-1,s)}$ or, equivalently, that the second term in the right-hand side of this equation cancels the Hermitian subset $R^{(s-1)}$ of $H^{(s-1,s)}$, which contains the physically unimportant terms. Consequently, the operator $S^{(s)}$ is obtained as the solution of

$$[S^{(s)}, H^{(0,0)}] = -R^{(s-1)} \tag{2.11}$$

while the sum of the physically important terms up to order s, that is,

$$K^{(s)} = \sum_{k=0}^{s} H^{(s,k)} = \sum_{k=0}^{s} H^{(k,k)} \tag{2.12}$$

is called the perturbative Hamiltonian of order s. Although some authors call $K^{(s)}$ the *effective* Hamiltonian of order s, we prefer to reserve this latter terminology for Hamiltonians that are formally similar to the perturbative Hamiltonians but whose coefficients have been obtained from fits against experimental data rather than from CPT.

It is important to realize that the choice of $H^{(0,0)}$ is of crucial importance, because the possibility of solving (2.11) with reasonable effort is governed by this choice. The remaining adjustment possibilities of the procedure in (2.8)–(2.11) are (*i*) the partition of the initial Hamiltonian $H^{(0)} = H$ into each of the $H^{(0,k)}$'s and (*ii*) the choice of the terms of $H^{(s-1,s)}$ that should be put into $R^{(s-1)}$ to be cancelled by the transformation at order s. How these adjustments are best performed for studying the highly excited vibrational dynamics of molecules with a single or several equilibrium positions as well as the dynamics on coupled electronic surfaces will be the subjects of the next three sections.

3. Application to semi-rigid molecules

This section is devoted to the application of CPT for the study of the highly excited vibrational dynamics of molecules with a single equilibrium position. Use of CPT for analyzing the low-energy portion of the spectrum has already attracted much attention (see, for example, refs. 3, 5–8, 27), while its application to the intermediate-energy spectrum has principally been investigated by Sibert and co-workers [9–12,28,38–43], Reinhardt and co-workers [44–48], and Sohlberg and Shirts [49]. We shall, therefore, lay emphasis on the specificity of high-energy perturbative calculations, i.e., the need for a careful choice of terms to be put in the successive $R^{(s-1)}$'s to insure convergence up to high orders of theory. As in refs. 13 and 17, the ab initio surface for HCP and the associated rotationless bound states calculated by Schinke and co-workers [50,51] will be used for the purpose of illustration.

As explained in Sect. 2, the classical ab initio Hamiltonian (expressed in terms of curvilinear internal coordinates [17]) is first expanded in a Taylor series in the neighborhood of the equilibrium position and then symmetrized. The polynomial obtained is then rewritten in terms of conjugate sets of dimensionless normal coordinates (p_j, q_j) by using Wilson et al.'s GF method [52] (q_j is the position coordinate and $p_j = -\mathrm{i}\partial/\partial q_j$ is its conjugate momentum). The goal of this linear canonical transformation is to rewrite the quadratic part of the expansion as a sum of uncoupled harmonic oscillators (see (3.4) below). One next converts the Hamiltonian to creation and annihilation operators, according to

$$\begin{aligned} q_j &= \frac{1}{\sqrt{2}}(a_j^+ + a_j) \\ p_j &= \frac{\mathrm{i}}{\sqrt{2}}(a_j^+ - a_j) \end{aligned} \tag{3.1}$$

for nondegenerate coordinates, like the CH stretch (mode $j = 1$) and the CP stretch (mode $j = 3$) of

HCP, and

$$\begin{aligned} q_j^2 &= a_{jg}^+ a_{jg} + a_{jd}^+ a_{jd} + a_{jg}^+ a_{jd}^+ + a_{jg} a_{jd} + 1 \\ p_j^2 &= a_{jg}^+ a_{jg} + a_{jd}^+ a_{jd} - a_{jg}^+ a_{jd}^+ - a_{jg} a_{jd} + 1 \\ q_j p_j &= \mathrm{i}\,(a_{jg}^+ a_{jd}^+ - a_{jg} a_{jd}) \end{aligned} \tag{3.2}$$

for doubly degenerate coordinates, like the bend (mode $j = 2$) of HCP. In (3.2), the operators a_{jd} and a_{jg} are defined as $(a_{jx} - \mathrm{i}\, a_{jy})/\sqrt{2}$ and $(a_{jx} + \mathrm{i}\, a_{jy})/\sqrt{2}$, respectively, while the subscripts d and g stand for "droit" (right) and "gauche" (left), because application of a_{jd} (respectively, a_{jg}) increases (repectively, decreases) by $\hbar$ the vibrational angular momentum. It should be recalled that the commutation relations involving these operators gives

$$\begin{aligned} [a_i, a_j] &= 0 \\ [a_i, a_j^+] &= \delta_{ij} \end{aligned} \tag{3.3}$$

where δ_{ij} is Kronecker's symbol and i and j take the values $1, 2g, 2d$, and 3 for HCP. One then proceeds to the partition of the initial Hamiltonian by putting each term with total degree $k+2$ in $H^{(0,k)}$, so that

$$\begin{aligned} H^{(0,0)} &= \sum_j \omega_j (a_j^+ a_j) \\ H^{(0,k)} &= \sum_{\|\boldsymbol{m}+\boldsymbol{n}\|=k+2} h^{(0)}_{\boldsymbol{mn}} \prod_j (a_j^+)^{m_j} (a_j)^{n_j} \qquad (k \geq 1) \end{aligned} \tag{3.4}$$

where the ω_j's are the fundamental frequencies, $\boldsymbol{m} = (m_1, m_2, \ldots)$ and $\boldsymbol{n} = (n_1, n_2, \ldots)$ are two vectors of positive integers, $\|\boldsymbol{m} + \boldsymbol{n}\|$ is the sum $m_1 + n_1 + m_2 + n_2 + \ldots$, and $h^{(0)}_{\boldsymbol{mn}}$'s are real coefficients that satisfy $h^{(0)}_{\boldsymbol{mn}} = h^{(0)}_{\boldsymbol{nm}}$. With this definition of $H^{(0,0)}$, the solution of (2.11) turns out to be very simple. Indeed, if the Hermitian subset $R^{(s-1)}$ of $H^{(s-1,s)}$ to be cancelled at order s of the perturbation procedure is of the form

$$R^{(s-1)} = \sum_{\|\boldsymbol{m}+\boldsymbol{n}\|=s+2} c^{(s-1)}_{\boldsymbol{mn}} \prod_j (a_j^+)^{m_j} (a_j)^{n_j} \tag{3.5}$$

where $c^{(s-1)}_{\boldsymbol{mn}}$ are real coefficients, then the solution of (2.11) is just

$$S^{(s)} = \sum_{\|\boldsymbol{m}+\boldsymbol{n}\|=s+2} \frac{c^{(s-1)}_{\boldsymbol{mn}}}{\sum_j (m_j - n_j)\omega_j} \prod_j (a_j^+)^{m_j} (a_j)^{n_j} \tag{3.6}$$

(note that $S^{(s)}$ is indeed anti-Hermitian). We now have at hand all the theoretical tools for applying CPT to the study of highly excited dynamics of semi-rigid molecules. Let us, however, emphasize, as noted by Sibert [9], that "a crucial feature of the computational procedure is that all the operators be expressed in a single form". Like Sibert, we have chosen to write all the creation operators first, as in (3.4)–(3.6). Evaluation of the commutators in (2.10) requires that many terms of the form $(a_j^+)^{m_j} (a_j)^{n_j} (a_j^+)^{m'_j} (a_j)^{n'_j}$ be rewritten in standard form. This is readily accomplished by using Sibert's formula given in eq. (2.11) of ref. 9.

The principal point one can play with to favor the convergence of the perturbation series is the choice, at each order s of the perturbation procedure, of the terms of $H^{(s-1,s)}$ to keep in $H^{(s,s)}$ or, conversely, to put in $R^{(s-1)}$ to be cancelled. Examination of (3.6) shows that terms of $H^{(s-1,s)}$ with $\boldsymbol{m} = \boldsymbol{n}$ must necessarily be kept in $H^{(s,s)}$ for the denominator not to diverge. The simplest perturbative

Fig. 1. Plot of the arithmetic average error between the energies of the eigenstates of HCP obtained from "exact" variational calculations [50,51] and from perturbative ones versus perturbation order s. The results for the Dunham expansions of (3.8) are indicated by squares, those for the Fermi-resonance Hamiltonians of (3.10) by lozenges, and those for the Hamiltonians with three resonances by circles. These latter Hamiltonians include the Fermi resonance $2\omega_2 - \omega_3 \approx 0$, its first harmonics $4\omega_2 - 2\omega_3 \approx 0$, and the additional resonance $2\omega_2 \approx 0$. Included in the calculations are the first 323 states of HCP, with energies up to 17 700 cm^{-1} above the quantum mechanical ground state, i.e., more than 75% of the energy of the CPH saddle. These levels contain up to $v_2 = 30$ quanta of excitation in the bend degree of freedom.

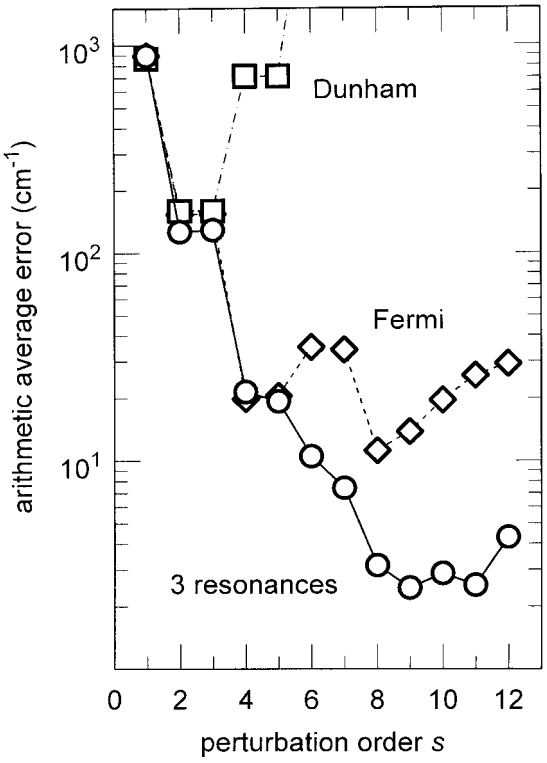

Hamiltonian is obtained by putting all the other terms in $R^{(s-1)}$. After s transformations, one is thus left with a perturbative Hamiltonian of the form

$$K^{(s)} = \sum_{\|\boldsymbol{m}\| \le s/2+1} h^{(s)}_{\boldsymbol{mm}} \prod_j (a_j^+)^{m_j} (a_j)^{m_j} \tag{3.7}$$

Upon linear expansion of each $(a_j^+)^{m_j}(a_j)^{m_j}$ operator in terms of the $(a_j^+ a_j)^{m_j}$ ones, the perturbative Hamiltonian can be written

$$K^{(s)} = K_{\mathrm{D}}^{(s)} = \sum_j v_j^{(s)} (a_j^+ a_j) + \sum_{j \le k} x_{jk}^{(s)} (a_j^+ a_j)(a_k^+ a_k) + \ldots \tag{3.8}$$

where the right-hand side of (3.8) contains terms with total degree up to $s + 2$. This is just the well-known Dunham polynomial expansion. Since $a_j^+ a_j |v_j\rangle = v_j |v_j\rangle$, the Dunham expansion is diagonal in the direct product basis of harmonic oscillators. The convergence properties of the series of Dunham Hamiltonians are illustrated in Fig. 1, where the arithmetic average error between the energies of the exact states of HCP [50,51] and those obtained from perturbation procedure are plotted as a function of the perturbation order s. Included in the calculations are the first 323 states of HCP, with energies up to

17 700 cm^{-1} above the quantum mechanical ground state, which is more than 75% of the energy of the CPH saddle. These levels contain up to 30 quanta of excitation in the bend degree of freedom. It can be seen from Fig. 1 that perturbation calculations diverge for orders s larger than 3, although the average arithmetic error at order $s = 3$ is still as large as 159 cm^{-1}.

When looking at the shape of the wave functions [50,51] and at the fundamental frequencies of HCP ($\omega_1 = 3479$ cm^{-1}, $\omega_2 = 650$ cm^{-1}, and $\omega_3 = 1256$ cm^{-1}), one realizes that this early divergence of the perturbation series is probably due to a Fermi resonance between the bend (mode 2) and the CP stretch (mode 3). One says that the fundamental frequencies are approximately resonant if there exist two vectors $\boldsymbol{m}^*$ and $\boldsymbol{n}^*$ of positive integers, such that

$$\sum_j (m_j^* - n_j^*)\omega_j \approx 0 \tag{3.9}$$

According to (3.6), the operators $S^{(s)}$ and the perturbation series diverge if the terms of $H^{(s-1,s)}$ such that $\boldsymbol{m} - \boldsymbol{n} = \pm(\boldsymbol{m}^* - \boldsymbol{n}^*)$ are put in $R^{(s-1)}$ when the resonance condition of (3.9) is satisfied. Therefore, these terms must necessarily be kept in $H^{(s,s)}$. After linear expansion of each $(a_j^+)^{m_j}(a_j)^{m_j}$ operator in terms of the $(a_j^+ a_j)^{m_j}$ ones, the perturbative Hamiltonian is thus obtained in the form

$$\begin{aligned} K^{(s)} &= K_{\mathrm{D}}^{(s)} + K_{\mathrm{R}}^{(s)} \\ K_{\mathrm{R}}^{(s)} &= \left\{ \prod_j (a_j^+)^{m_j^*} \right\} \left\{ k^{(s)} + \sum_j k_j^{(s)} (a_j^+ a_j) + \sum_{j \leqslant k} k_{jk}^{(s)} (a_j^+ a_j)(a_k^+ a_k) + \ldots \right\} \left\{ \prod_j (a_j)^{n_j^*} \right\} \end{aligned} \tag{3.10}$$

where $K_{\mathrm{D}}^{(s)}$ is the Dunham expansion of (3.8) and the right-hand side of the second equation again contains terms with total degree up to $s + 2$. It is of course possible to take two (or more) resonances simultaneously into account. When doing so, the perturbative Hamiltonian $K^{(s)}$ consists of the Dunham expansion $K_{\mathrm{D}}^{(s)}$ plus two (or more) resonance terms $K_{\mathrm{R}}^{(s)}$. It should, however, be kept in mind that each additional linearly independent resonance destroys one good quantum number and consequently increases the size of the matrices to be diagonalized. Moreover, from the dynamical point of view, the Hamiltonians with two (or more) independent resonances are at least partially chaotic, while those with zero or one resonance are completely integrable and, therefore, best suited for the purpose of semiclassical investigations.

Because of the degeneracy of the bending motion, the Fermi resonance $2\omega_2 - \omega_3 \approx 0$ between the bend (mode 2) and the CP stretch (mode 3) of HCP is described by the vectors $\boldsymbol{m}^* = (m_1^*, m_{2g}^*, m_{2d}^*, m_3^*) = (0, 1, 1, 0)$ and $\boldsymbol{n}^* = (n_1^*, n_{2g}^*, n_{2d}^*, n_3^*) = (0, 0, 0, 1)$. Since both v_1 (the number of quanta in the CH stretch) and $P = v_2 + 2v_3$ (P is called the polyad number) are good quantum numbers for the Fermi-resonance Hamiltonian (i.e., the perturbative Hamiltonian with the $2\omega_2 - \omega_3 \approx 0$ resonance), the eigenstates are obtained from the diagonalization of very small matrices of size $P/2 + 1$ [13,15,53]. The convergence properties of the series of Fermi-resonance Hamiltonians are illustrated in Fig. 1. It can be seen that they perform much better than the Dunham expansions because convergence is obtained up to 8th order of the theory. At this order, the average arithmetic error is 11.2 cm^{-1}. A closer examination of exact and perturbative energies reveals that a vast majority of states are accurately reproduced by the Fermi-resonance Hamiltonian, while a dozen states with $v_2 \geq 22$ have considerably larger errors that range up to 394 cm^{-1}.

A systematic search for additional resonances must next be undertaken to improve the calculation of the states with the largest values of v_2. Note that, according to (3.6), it is not necessarily the resonances with the smallest values of $\sum_j (m_j^* - n_j^*)\omega_j$ that prove to be important, but instead those with the largest values of $c_{\boldsymbol{mn}}^{(s-1)} / \sum_j (m_j^* - n_j^*)\omega_j$. It turns out that excellent results are obtained upon simultaneous introduction in the perturbative Hamiltonian of the first harmonics $4\omega_2 - 2\omega_3 \approx 0$ of the Fermi resonance,

Fig. 2. Plot of the difference between exact and perturbative quantum energies for the first 323 states of HCP at 9th (top plot) and 11th (bottom plot) order of the theory versus energy of each state. The perturbative Hamiltonians take the three resonances $2\omega_2 - \omega_3 \approx 0$, $4\omega_2 - 2\omega_3 \approx 0$, and $2\omega_2 \approx 0$ into account. At order $s = 9$, the error for the lowest state of polyad $[v_1, P] = [0, 30]$, which is calculated at 95 cm^{-1}, lies out of the plotting range. At order $s = 11$, the errors for the lowest state of polyads [0,26], [0,28], [0,30], and [1,24], as well as for the second lowest state of polyad [0,30], which are calculated at 36, 111, 191, 20, and 51 cm^{-1}, respectively, lie out of the plotting range.

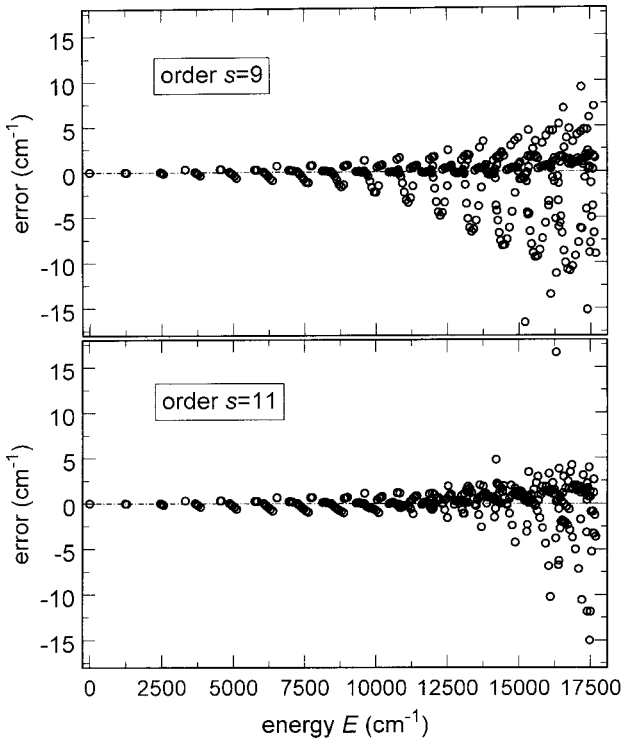

which is characterized by the vectors $\boldsymbol{m}^* = (0, 2, 2, 0)$ and $\boldsymbol{n}^* = (0, 0, 0, 2)$, and the $2\omega_2 \approx 0$ resonance with vectors $\boldsymbol{m}^* = (0, 1, 1, 0)$ and $\boldsymbol{n}^* = (0, 0, 0, 0)$. When taking the three resonances into account, there is only one good quantum number left, namely, v_1, the number of quanta in the CH stretch, but the size of the matrices to diagonalize still remains very small compared with exact quantum calculations. As can be checked in Fig. 1, the convergence properties of the three-resonance Hamiltonians are again substantially better than those of the Fermi-resonance Hamiltonians. As shown in the upper panel of Fig. 2, an average error as small as 2.45 cm^{-1} is obtained at order $s = 9$, with only one error larger than 20 cm^{-1}, that for the state with the maximum number of quanta ($v_2 = 30$) in the bend. Comparison of the two panels of Fig. 2 further shows that the errors for most states are again substantially reduced when s increases from $s = 9$ to 11. Unfortunately, the errors for the four states with the largest values of v_2 diverge again, so that the average error remains nearly constant. The divergence for the states with the largest values of v_2 is here principally because the polynomial Taylor expansion fails to correctly reproduce the potential-energy surface for the largest values of the bending angle.

It is interesting to note that convergence properties very close to those of the three-resonance Hamiltonians are obtained when computing the eigenstates of the Fermi-resonance Hamiltonians, but with the parameters $\nu_j^{(s)}, x_{jk}^{(s)}, \ldots, k^{(s)}, k_j^{(s)}, \ldots$ of the three-resonance Hamiltonians [17]. The semiclassical analysis of this latter Fermi-resonance Hamiltonian provides unparalleled insight into the highly excited vibrational dynamics of HCP and particularly into the saddle-node bifurcation, which is the first step of the HCP↔CPH isomerization process [13,15,16,53].

Fig. 3. Contour plot of typical potential-energy surface of a floppy molecule. The black dots at $\gamma = 0°$ and 180° denote the two equilibrium positions, while the black dot around $\gamma = 95°$ indicates a saddle. The dotted line is the minimum energy path, which connects the three extrema. The coordinate γ (vertical axis in degrees) is called a reactive coordinate and the coordinate R (horizontal axis in Angstroms) an inactive one.

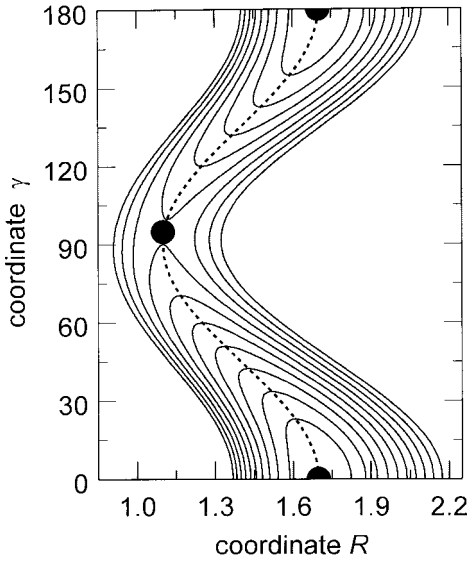

4. Application to floppy molecules

This section is devoted to the application of CPT to the study of the highly excited vibrational dynamics of floppy molecules. The procedure described below is an improved version of the work published in refs. 14 and 18. As in this earlier work, the ab initio surface for HCN computed by Murrell et al. [54] and the corresponding rotationless bound states calculated by Bacic [55] will be used for the purpose of illustration.

The typical potential-energy surface of floppy molecules is shown in Fig. 3. It is characterized by the existence of at least two equilibrium positions, which are separated by saddle points. A "minimum energy path" (MEP), also called a "reaction pathway", connects the different equilibrium positions and the saddles. In Fig. 3, the equilibrium positions are the two black dots at $\gamma = 0°$ and 180°, the saddle is the black dot at about $\gamma = 95°$, and the reaction pathway is the dotted line. The perturbative Hamiltonian we are looking for must accurately reproduce the states of the initial Hamiltonian in both wells up to and above the isomerization barrier. It is clearly seen in Fig. 3 that the vibrational degrees of freedom can be separated into two different families. The first family includes those coordinates whose variation leads from one well to another well and which will, therefore, be called "reactive coordinates". The second family includes all the other coordinates whose variation remains localized in one well and which will henceforth be described as "inactive coordinates". Coordinate γ of Fig. 3 is a reactive coordinate, while R is an inactive one. In most cases, the dynamics of small floppy molecules involves a single reactive coordinate (generally an angle) and several inactive ones. For example, the two Jacobi coordinates r and R behave as inactive coordinates for the HCN $\leftrightarrow$ CNH isomerization reaction, while the Jacobi angle γ is the reactive coordinate (r is the CN bond length, R the distance between H and the center of mass G of CN, and γ the HGN angle).

There exist at least two reasons why the procedure described in the previous section cannot be used to study the dynamics of floppy molecules. First, the Taylor expansion in the neighborhood of one equilibrium position is expected to describe correctly the corresponding well, but certainly not two (or more) of them. Moreover, treating a reactive mode as if it were an harmonic oscillator is bound to fail, since it behaves much more like a hindered rotor in the neighborhood of the isomerization saddle and like

a free rotor largely above the saddle. Inspired by the previous works of Marcus [56–58], Miller and co-workers [59–61], and Chapuisat and co-workers [62–66], we have found that an excellent approximation of the ab initio Hamiltonian is obtained from a mixed expansion of the ab initio Hamiltonian around the MEP. The first step for obtaining this expansion consists of a canonical transformation, according to

$$\begin{aligned} q_j &\rightarrow q_j^0(\gamma) + z_j \\ \frac{\partial}{\partial \gamma} &\rightarrow \frac{\partial}{\partial \gamma} - \sum_j \frac{\mathrm{d}q_j^0(\gamma)}{\mathrm{d}\gamma} \frac{\partial}{\partial z_j} \end{aligned} \tag{4.1}$$

where a single reactive coordinate γ has been assumed and the index j is restricted to inactive coordinates q_j, that is, to $j = 1$ (CN stretch) and $j = 3$ (CH stretch) in the case of the HCN molecule. $q_j^0(\gamma)$ is the value of q_j on the MEP for each particular value of γ. The Hamiltonian obtained is then Taylor-expanded relative to z_j's and z_j the deviation of q_j from $q_j^{(0)}(\gamma)$ for this particular value of γ and Fourier-expanded relative to the reactive coordinate γ (for more details on the technical procedure, see ref. 18). Practically, the ab initio Hamiltonian for the HCN $\leftrightarrow$ CNH system [54] was Fourier expanded up to $\cos(10\gamma)$. The expression obtained was next rewritten in terms of powers of $\cos\gamma$. Note that all the powers of $\cos\gamma$ that appear in the course of the calculations must be retained, even when larger than 10, for the perturbative Hamiltonian to remain Hermitian. With the initial partition described below, the maximum power of $\cos\gamma$ increases like $10(s-2)$. After conversion of the z_j's and their conjugate momenta to creation–annihilation operators (cf. (3.1)–(3.2)), the initial Hamiltonian is thus of the form

$$H^{(0)} = \sum_{M,P,N,\boldsymbol{m},\boldsymbol{n}} h^{(0)}_{MPN\boldsymbol{mn}} (\cos\gamma)^M \sigma^P (J^2)^N \prod_j (a_j^+)^{m_j} (a_j)^{n_j} \tag{4.2}$$

where j is restricted to inactive coordinates. The $h^{(0)}_{MPN\boldsymbol{mn}}$'s are real coefficients. σ denotes the operator $\sin\gamma \frac{\partial}{\partial\gamma}$. The associated exponent P can take only the values 0 and 1 (note that P has nothing to do with the polyad number defined in Sect. 3). J^2 stands for the operator

$$J^2 = -\frac{1}{\sin\gamma} \frac{\partial}{\partial\gamma} \sin\gamma \frac{\partial}{\partial\gamma} - \frac{1}{(\sin\gamma)^2} \frac{\partial^2}{\partial\varphi^2} \tag{4.3}$$

where φ is the rotation angle around the axis of inertia with smallest momentum. The matrix elements of these operators in the basis of the spherical functions $|\ell, m\rangle = Y_\ell^m(\gamma, \varphi)$ are easily obtained from

$$\begin{aligned} J^2|\ell,m\rangle &= \ell(\ell+1)\,|\ell,m\rangle \\ \sigma|\ell,m\rangle &= \ell\sqrt{\frac{(\ell-m+1)(\ell+m+1)}{(2\ell+1)(2\ell+3)}}|\ell+1,m\rangle - (\ell+1)\sqrt{\frac{(\ell-m)(\ell+m)}{(2\ell-1)(2\ell+1)}}|\ell-1,m\rangle \\ \cos\gamma|\ell,m\rangle &= \sqrt{\frac{(\ell-m+1)(\ell+m+1)}{(2\ell+1)(2\ell+3)}}|\ell+1,m\rangle + \sqrt{\frac{(\ell-m)(\ell+m)}{(2\ell-1)(2\ell+1)}}|\ell-1,m\rangle \end{aligned} \tag{4.4}$$

The form of $H^{(0)}$ in (4.2) is thus particularly suitable for energy level calculations and will be preserved for each $H^{(s)}$ by the successive transformations. Note that the major advantage of the method presented here lies precisely in the fact that states with different values of the vibrational angular are treated simultaneously and on the same footing, while the older version of refs. 14 and 18 required additional hard work for the states with $m > 0$. As for semi-rigid molecules, it is of practical importance to express all the operators in a single standard form, which is chosen to be that of (4.2). Evaluation of the commutators in (2.10) then requires that many terms of the form $(\cos\gamma)^M \sigma^P (J^2)^N (\cos\gamma)^{M'} \sigma^{P'} (J^2)^{N'}$

be rewritten in the standard form. We did not try to derive a general formula, like Sibert for creation–annihilation operators [9]. Each product is instead iteratively recast in the normal form by using the following fundamental relations:

$$
\begin{aligned}
J^2(\cos\gamma)^M &= (\cos\gamma)^M J^2 + 2M(\cos\gamma)^{M-1}\sigma + M(M+1)(\cos\gamma)^M - M(M-1)(\cos\gamma)^{M-2} \\
J^2(\cos\gamma)^M\sigma &= (\cos\gamma)^M\sigma J^2 + 2(M+1)(\cos\gamma)^{M+1}J^2 - 2M(\cos\gamma)^{M-1}J^2 \\
&\qquad + M(M+1)(\cos\gamma)^M\sigma - M(M-1)(\cos\gamma)^{M-2}\sigma \\
\sigma(\cos\gamma)^M &= (\cos\gamma)^M\sigma + M(\cos\gamma)^{M+1} - M(\cos\gamma)^{M-1} \\
\sigma(\cos\gamma)^M\sigma &= (\cos\gamma)^{M+2}J^2 - (\cos\gamma)^M J^2 + M(\cos\gamma)^{M+1}\sigma - M(\cos\gamma)^{M-1}\sigma
\end{aligned}
\tag{4.5}
$$

A crucial question concerns the partition of the initial Hamiltonian $H^{(0)}$ into the various $H^{(0,k)}$'s and particularly the terms to be put into $H^{(0,0)}$. Since the resolution of (2.11) turns out to be quite difficult if $H^{(0,0)}$ depends on the reactive coordinate, $H^{(0,0)}$ must be chosen to contain only the sum of the harmonic oscillators associated with the inactive modes, that is

$$H^{(0,0)} = \sum_j \omega_j (a_j^+ a_j) \tag{4.6}$$

where the index j is, however, restricted to inactive coordinates. When doing so, the solution of (2.11) is very similar to (3.5)–(3.6). Indeed, if

$$R^{(s-1)} = \sum_{M,P,N,\boldsymbol{m},\boldsymbol{n}} c^{(s-1)}_{MPN\boldsymbol{mn}} (\cos\gamma)^M \sigma^P (J^2)^N \prod_j (a_j^+)^{m_j} (a_j)^{n_j} \tag{4.7}$$

then the solution of (2.11) is just

$$S^{(s)} = \sum_{M,P,N,\boldsymbol{m},\boldsymbol{n}} \frac{c^{(s-1)}_{MPN\boldsymbol{mn}}}{\sum_j \omega_j (m_j - n_j)} (\cos\gamma)^M \sigma^P (J^2)^N \prod_j (a_j^+)^{m_j} (a_j)^{n_j} \tag{4.8}$$

where the index j is again restricted to inactive modes. There is more freedom for the ordering of the other terms. We found that a good choice, which warrants both rapid calculations and convergence up to high orders, consists in putting each term with indices M, P, N, $\boldsymbol{m}$ and $\boldsymbol{n}$ into $H^{(0,k)}$, where $k = \|\boldsymbol{m}+\boldsymbol{n}\| + P + 2N - 2$ if $M = 0$ and $k = \|\boldsymbol{m}+\boldsymbol{n}\| + P + 2N$ if $M > 0$. An exception obviously occurs for the pure bending terms J^2 and $\cos^M(\gamma)$, which are put into $H^{(0,1)}$ instead of $H^{(0,0)}$. Each $H^{(0,k)}$ is symmetrized after partition has been completed. Be careful that σ is not exactly antisymmetric, but satisfies instead

$$\sigma^+ = -\sigma - 2\cos\gamma \tag{4.9}$$

One now has all the necessary tools handy for studying floppy molecules. The question that naturally arises concerns the form of the perturbative Hamiltonian, that is, of the terms of $H^{(s-1,s)}$ to keep in $H^{(s,s)}$ or, conversely, to put in $R^{(s-1)}$ to be cancelled by the perturbation procedure. The simplest perturbative Hamiltonian is the one for which the number of quanta in each inactive mode remains a good quantum number. It is obtained by putting each term with indices M, P, N, $\boldsymbol{m}$, and $\boldsymbol{n}$ ($\boldsymbol{m} \neq \boldsymbol{n}$) into $R^{(s-1)}$. After linear expansion of each $(a_j^+)^{m_j}(a_j)^{m_j}$ operator in terms of the $(a_j^+ a_j)^{m_j}$ ones, the perturbative Hamiltonian is thus obtained in the form

$$K^{(s)} = \sum_{M,P,N,\boldsymbol{m}} k^{(s)}_{MPN\boldsymbol{m}} (\cos\gamma)^M \sigma^P (J^2)^N \prod_j (a_j^+ a_j)^{m_j} \tag{4.10}$$

Fig. 4. Plot of the arithmetic average error between the energies of the eigenstates of HCN obtained from exact variational calculations [55] and from perturbative calculations versus perturbation order s. The perturbative Hamiltonian, defined in (4.10), is formally a one-dimensional Hamiltonian (in the reactive coordinate γ) parametrized by the number of quanta in the CH and CN stretches. Included in the calculations are the first 111 states of the HCN $\leftrightarrow$ CNH system, with energies up to 11 770 cm^{-1} above the quantum mechanical ground state, that is, slightly above the isomerization saddle for pure bending states. These levels contain up to $v_2 = 44$ quanta of excitation in the bend degree of freedom.

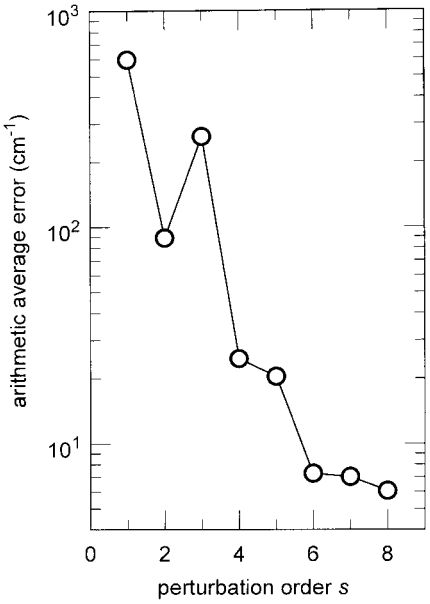

Equation (4.10) is the counterpart of the Dunham expansion of (3.8) for floppy molecules. The convergence properties of this perturbative series are illustrated in Fig. 4, where the arithmetic average error between the energies of the exact states of HCN [55] and those obtained from the perturbative Hamiltonians of (4.10) are plotted as a function of the perturbation order s. Included in the calculations are the first 111 states of the HCN $\leftrightarrow$ CNH system, with energies up to 11 770 cm^{-1} above the quantum mechanical ground state, that is, slightly above the barrier to linearity for pure bending states (two states are almost uniformly delocalized over the two wells). Note that we stopped comparison with exact quantum results at this energy because of the lack of reliable quantum results for larger values of the bend quantum number and not because of an abrupt degradation of the accuracy of the perturbative Hamiltonian. It can be seen in Fig. 4 that the perturbation series converges rapidly up to order $s = 6$ before remaining stationary at orders $s = 7$ and 8. At order $s = 6$, very small $|\ell, m\rangle$ bases with $0 \leqslant \ell \leqslant 48$ and $m = 0$ result in computed perturbative energies, which vary by less than 10^{-3} cm^{-1} upon further increase of the basis size. It can furthermore be checked in Fig. 5 that the error between the energies of exact and perturbative (6th order) quantum states increases smoothly with energy, although a few pairs of more resonantly coupled states are observed at the highest energies, i.e., close to the isomerization saddle for pure bending states.

The perturbative Hamiltonian of (4.10) is formally a one-dimensional system (in the reactive coordinate) parametrized by the number of quanta $v_j = a_j^+ a_j$ in the inactive modes $j = 1$ (CN stretch) and $j = 3$ (CH stretch). An illustration thereof is provided in Fig. 6, which shows the pseudo-potential curve and the probability density for the pure bending states of HCN. The pseudo-potential curve is obtained by setting J, σ, $v_1 = a_1^+ a_1$, and $v_3 = a_3^+ a_3$ to zero in (4.10). Being one-dimensional, the perturbative Hamiltonian is necessarily integrable (i.e., non-chaotic). From the physical point of view, it is interesting to note that the "exact" HCN $\leftrightarrow$ CNH system remains very close to the integrable

Fig. 5. Plot of the difference between exact and perturbative quantum energies for the first 111 states of HCN at 6th order of the theory versus energy of each state. The perturbative Hamiltonian is that of (4.10).

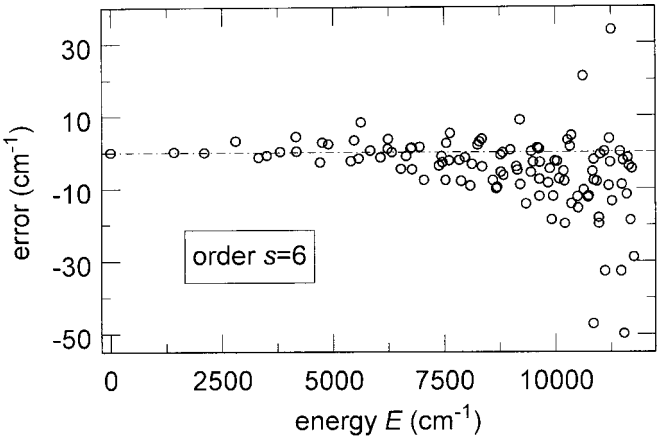

Fig. 6. Plot of the pseudo-potential (thick line) and the probability density (thinner lines) for the pure bending states ($v_1 = v_3 = 0$) of the HCN $\leftrightarrow$ CNH system versus bending angle γ. These results are obtained by applying 6th-order CPT to the ab initio surface of Murrell et al. [54]. The energies on the vertical axis are plotted relative to the minimum of the potential-energy surface. The vertical scale is the same for all probability plots and the baseline for each plot coincides, on the vertical axis, with the energy of the corresponding state.

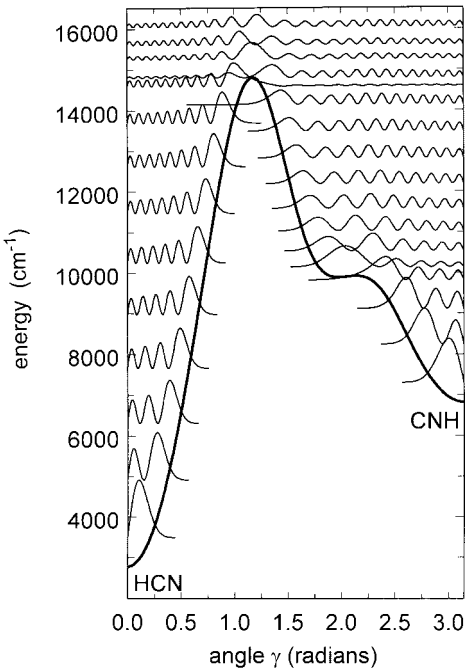

perturbative Hamiltonian, even in the region close to the saddle where classical dynamics is known to be largely chaotic. A similar situation was encountered while studying the dynamics of HOCl close to the dissociation threshold [67]. It was indeed found that an integrable Fermi-resonance Hamiltonian accurately reproduces the dynamics of the exact system in this largely chaotic region of the phase space (see also refs. 16, 23, 44–49).

5. Application to non-Born–Oppenheimer dynamics

This section is devoted to the application of CPT to the study of non-Born–Oppenheimer dynamics, that is, of vibrationally excited molecules on coupled electronic surfaces. The procedure described below is a simplified version of the work published in ref. 19. A still different scheme is presented in ref. 20 but will not be discussed in this article because it does not follow the general lines of Sect. 2. As in refs. 19 and 20, a simple model with two 2-dimensional diabatic electronic surfaces coupled by a linear term will serve for the purpose of illustration, although the conclusions derived from refs. 19 and 20 have recently been used to get a precise model of the conical intersection in NO_2 [68].

The diabatic vibronic Hamiltonian of a molecular system with two coupled electronic surfaces can be written as

$$\boldsymbol{H} = \begin{pmatrix} T + V_e & V_c \\ V_c & T + V_g \end{pmatrix} \tag{5.1}$$

where T is the kinetic energy of the molecule and V_g, V_e, and V_c are the diabatic ground, excited, and coupling surfaces, respectively. As in refs. 19 and 20, one takes

$$\begin{aligned} T &= \frac{1}{2}\omega_{1g}p_1^2 + \frac{1}{2}\omega_{2g}p_2^2 \\ V_g &= \frac{1}{2}\omega_{1g}q_1^2 + \frac{1}{2}\omega_{2g}q_2^2 \\ V_e &= \Delta E + \frac{1}{2}\frac{\omega_{1e}^2}{\omega_{1g}}(q_1 - q_{10})^2 + \frac{1}{2}\frac{\omega_{2e}^2}{\omega_{2g}}(q_2 - q_{20})^2 \\ V_c &= \lambda q_1 \end{aligned} \tag{5.2}$$

that is, the ground and excited surfaces are the sum of two uncoupled harmonic oscillators with center shift and frequency mismatch, while the coupling surface is just the linear term that is known to dominate the conical intersection of NO_2 and several other polyatomic molecules [69–74]. Note that the Hamiltonian in (5.2) is written in terms of the normal coordinates of the ground electronic surface V_g. As in refs. 19 and 20, numerical values are $\omega_{1g} = 1669\ \mathrm{cm}^{-1}$, $\omega_{2g} = 759\ \mathrm{cm}^{-1}$, $\omega_{1e} = 1000\ \mathrm{cm}^{-1}$, and $\omega_{2e} = 745\ \mathrm{cm}^{-1}$ for the fundamental frequencies of V_g and V_e, $\Delta E = 9700\ \mathrm{cm}^{-1}$ for the energy shift between the bottoms of the two surfaces, $q_{10} = 0$ and $q_{20} = 2$ for the center shift, and $\lambda = 700\ \mathrm{cm}^{-1}$ for the diabatic coupling (except for q_{20}, these values are close to those for the antisymmetric stretch and bend degrees of freedom of NO_2 in the two lowest electronic states). The contour plots of V_g and V_e are displayed in Fig. 7. Note that the bottom of the excited surface V_e lies inside the ground-state well. Figure 8 shows how the states of the uncoupled ground (circles) and excited (lozenges) surfaces are shifted upon switching on the diabatic coupling. The vertical line locates the energy of the bottom of V_e. It can be seen in this figure that the ground state of V_g is already shifted to lower energies by more than $20\ \mathrm{cm}^{-1}$ and that shifts may reach about $500\ \mathrm{cm}^{-1}$ close to the bottom of V_e. This is because each zero-order state of the uncoupled ground surface V_g is coupled through V_c to a large number of high-energy zero-order states of the uncoupled excited surface V_e, so that switching on the diabatic coupling V_c results in large shifts for all of the states of V_g and V_e, including those states of V_g located far below the bottom of V_e. Nonetheless, these shifts appear to be quite regular, which indicates that, in the investigated energy range, switching on the diabatic coupling V_c principally modifies the harmonic frequencies and the anharmonicities in each well. The goal of the remainder of this section is to show how these harmonic and anharmonic corrections are obtained from CPT.

For the sake of clarity, the case for $n = 2$ coupled electronic surfaces is handled explicitly here, but the procedure extends readily to larger values of n. One defines a n^2-dimensional basis ($\boldsymbol{g}$, $\boldsymbol{e}$, $\boldsymbol{j}_+$, $\boldsymbol{j}_-$) of $n \times n$ matrices

$$\boldsymbol{g} = \begin{pmatrix} 0 & 0 \\ 0 & 1 \end{pmatrix}, \qquad \boldsymbol{e} = \begin{pmatrix} 1 & 0 \\ 0 & 0 \end{pmatrix}, \qquad \boldsymbol{j}_+ = \begin{pmatrix} 0 & 1 \\ 0 & 0 \end{pmatrix}, \qquad \boldsymbol{j}_- = \begin{pmatrix} 0 & 0 \\ 1 & 0 \end{pmatrix} \tag{5.3}$$

Fig. 7. Contour plots of the ground V_g (continuous lines) and the excited V_e (broken lines) diabatic surfaces of (5.1) and (5.2). q_1 and q_2 are the dimensionless coordinates of the ground surface V_g. The contours range from 1500 to 18 000 cm^{-1} for V_g and from 10 500 to 18 000 cm^{-1} for V_e, with increments of 1500 cm^{-1}. The two black dots indicate the minimum of each surface. Note that the minimum of the excited electronic surface V_e lies inside the well of the ground surface V_g. The thicker line indicates the crossing seam between the two surfaces.

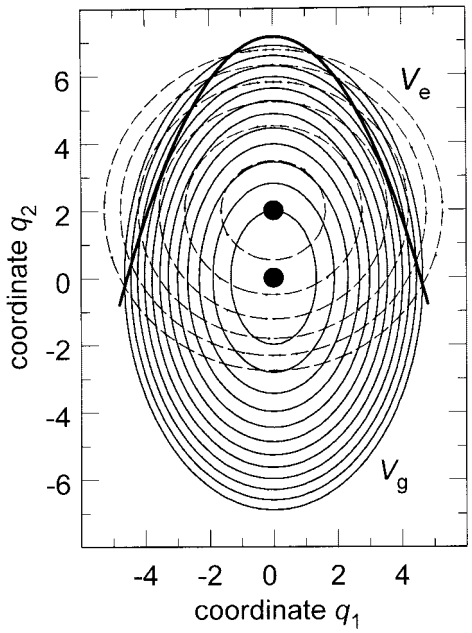

where $\boldsymbol{g}$ and $\boldsymbol{e}$ are the projections on the ground and excited surfaces, respectively, and $\boldsymbol{j}_+$ and $\boldsymbol{j}_-$ are raising- and lowering-like operators. Each operator $\boldsymbol{A}$ is decomposed on this basis according to

$$\boldsymbol{A} = \begin{pmatrix} A_e & A_+ \\ A_- & A_g \end{pmatrix} = A_g\,\boldsymbol{g} + A_e\boldsymbol{e} + A_+\boldsymbol{j}_+ + A_-\boldsymbol{j}_- \tag{5.4}$$

and the commutator $\boldsymbol{C} = [\boldsymbol{A}, \boldsymbol{B}] = \boldsymbol{AB} - \boldsymbol{BA}$ of two operators $\boldsymbol{A}$ and $\boldsymbol{B}$ can be written

$$\begin{aligned} C_g &= [A_g, B_g] + A_-B_+ - B_-A_+ \\ C_e &= [A_e, B_e] + A_+B_- - B_+A_- \\ C_+ &= A_+B_g - B_+A_g + A_eB_+ - B_eA_+ \\ C_- &= A_-B_e - B_-A_e + A_gB_- - B_gA_- \end{aligned} \tag{5.5}$$

As for the dynamics on a single electronic surface, the initial Hamiltonian $\boldsymbol{H}$ of (5.1) and (5.2) must be partitioned into $\boldsymbol{H}^{(0,0)}$ plus higher order terms $\boldsymbol{H}^{(0,k)}$ ($k \geq 1$) and the rules for obtaining the successive operators $\boldsymbol{S}^{(s)}$ from the unwanted terms of $\boldsymbol{H}^{(s-1,s)}$ must be found for each perturbation order s, except that all operators are now matrix quantities. For the transformations of (2.6) to be unitary ones, $S_g^{(s)}$ and $S_e^{(s)}$ must be anti-Hermitian, while $S_+^{(s)}$ and $S_-^{(s)}$ must satisfy

$$S_+^{(s)} = -S_-^{(s)^+} \tag{5.6}$$

where $S_g^{(s)}$, $S_e^{(s)}$, $S_+^{(s)}$, and $S_-^{(s)}$ are the components of $\boldsymbol{S}^{(s)}$ in the ($\boldsymbol{g}$, $\boldsymbol{e}$, $\boldsymbol{j}_+$, $\boldsymbol{j}_-$) basis. These conditions are automatically fulfilled by the procedure proposed below. Examination of the matrix version of (2.11)

$$[\boldsymbol{S}^{(s)}, \boldsymbol{H}^{(0,0)}] = -\boldsymbol{R}^{(s-1)} \tag{5.7}$$

Fig. 8. Plot of the energy shifts of the states belonging to the ground (circles) and excited (lozenges) diabatic surfaces caused by the coupling (through V_c) to the other surface versus absolute energy E of each state. The vertical line indicates the energy of the bottom of the excited surface V_e ($E = 9700$ cm^{-1}).

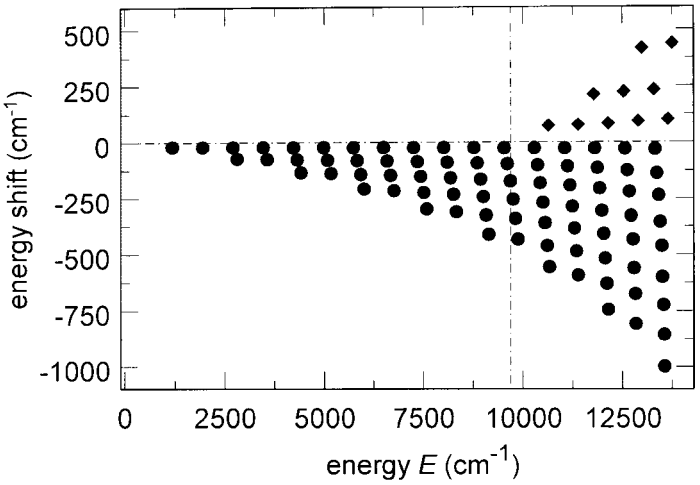

shows that $\boldsymbol{H}^{(0,0)}$ must satisfy severe constraints for this equation to be easy to solve. The best choice probably consists in taking

$$\boldsymbol{H}^{(0,0)} = \left(\frac{\omega_{1g}}{2}a_1^+a_1 + \frac{\omega_{2g}}{2}a_2^+a_2\right)\boldsymbol{g} + \left(\delta E + \frac{\omega_{1g}}{2}a_1^+a_1 + \frac{\omega_{2g}}{2}a_2^+a_2\right)\boldsymbol{e} \tag{5.8}$$

where

$$\delta E = \Delta E + \frac{\omega_{1e} + \omega_{2e}}{2} - \frac{\omega_{1g} + \omega_{2g}}{2} \tag{5.9}$$

is the energy gap between the ground states of V_g and V_e, and the (a_j^+, a_j) creation and annihilation operators are obtained from the normal coordinates (p_j, q_j) of the ground electronic surface V_g according to (3.1). All other terms, which describe the diabatic coupling as well as the frequency mismatch and the center shift between the two electronic surfaces, are put in $\boldsymbol{H}^{(0,1)}$. Investigation of more complex systems will probably require the ordering of (here missing) higher order terms of V_g, V_e, and V_c as in the lower equation of (3.4). The fact that all operators are expressed in terms of the creation and annihilation operators of the ground electronic surface V_g is the principal advantage of the formulation presented in this article when compared with the first version given in ref. 19. Indeed, in this earlier work, creation and annihilation operators referred to a virtual average surface $(V_g + V_e)/2$. Equation (5.7) is very easy to solve when $\boldsymbol{H}^{(0,0)}$ is taken as in (5.8). Indeed, if the Hermitian subset $\boldsymbol{R}^{(s-1)}$ of $\boldsymbol{H}^{(s-1,s)}$ to be cancelled at order s of the perturbation procedure is of the form

$$\begin{aligned}\boldsymbol{R}^{(s-1)} = \boldsymbol{g}\sum_{\boldsymbol{m},\boldsymbol{n}} a_{\boldsymbol{mn}}^{(s-1)}\prod_j (a_j^+)^{m_j}(a_j)^{n_j} + \boldsymbol{e}\sum_{\boldsymbol{m},\boldsymbol{n}} b_{\boldsymbol{mn}}^{(s-1)}\prod_j (a_j^+)^{m_j}(a_j)^{n_j} \\ + \boldsymbol{j}_+\sum_{\boldsymbol{m},\boldsymbol{n}} c_{\boldsymbol{mn}}^{(s-1)}\prod_j (a_j^+)^{m_j}(a_j)^{n_j} + \boldsymbol{j}_-\sum_{\boldsymbol{m},\boldsymbol{n}} d_{\boldsymbol{mn}}^{(s-1)}\prod_j (a_j^+)^{m_j}(a_j)^{n_j}\end{aligned} \tag{5.10}$$

Fig. 9. Plot of the arithmetic average error between the exact energies of the model Hamiltonian of (5.1) and (5.2) and those obtained from the perturbative Hamiltonian of (5.12) and (5.13) versus perturbation order s. The perturbative Hamiltonian consists of two uncoupled Dunham expansions, one for the ground electronic surface and another for the excited surface. Included in the calculations are the first 91 states of the system shown in Fig. 8, with energies up to 14 000 cm^{-1} above the minimum of V_g. Among these 91 states, 81 are principally localized on the V_g surface and 10 on the V_e surface. These states contain up to $v_2 = 16$ quanta of excitation in mode 2.

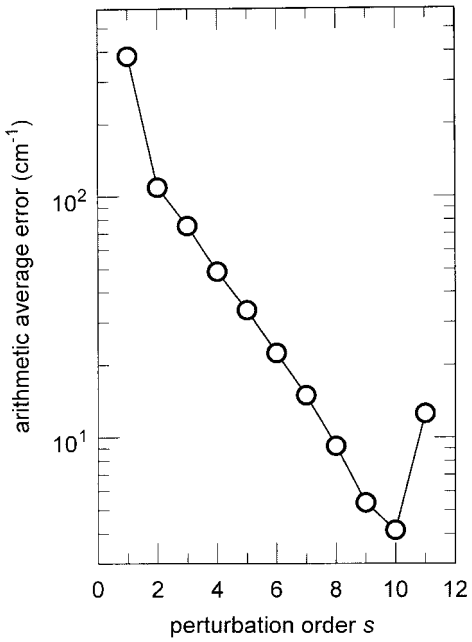

then the solution of (5.7) is just

$$\boldsymbol{S}^{(s)} = \boldsymbol{g}\sum_{\boldsymbol{m},\boldsymbol{n}} \frac{a_{\boldsymbol{mn}}^{(s-1)}}{\Sigma_{\boldsymbol{mn}}} \prod_j (a_j^+)^{m_j}(a_j)^{n_j} + \boldsymbol{e}\sum_{\boldsymbol{m},\boldsymbol{n}} \frac{b_{\boldsymbol{mn}}^{(s-1)}}{\Sigma_{\boldsymbol{mn}}} \prod_j (a_j^+)^{m_j}(a_j)^{n_j} + \boldsymbol{j}_+\sum_{\boldsymbol{m},\boldsymbol{n}} \frac{c_{\boldsymbol{mn}}^{(s-1)}}{\Sigma_{\boldsymbol{mn}} - \delta E} \prod_j (a_j^+)^{m_j}(a_j)^{n_j} + \boldsymbol{j}_-\sum_{\boldsymbol{m},\boldsymbol{n}} \frac{d_{\boldsymbol{mn}}^{(s-1)}}{\Sigma_{\boldsymbol{mn}} + \delta E} \prod_j (a_j^+)^{m_j}(a_j)^{n_j} \quad (5.11)$$

where $\Sigma_{\boldsymbol{mn}} = \sum_j (m_j - n_j)\,\omega_{jg}$. The simplest perturbative Hamiltonian one can think of consists of two Dunham expansions (one for the electronic ground state and one for the excited state) with no coupling between the two surfaces, that is

$$\boldsymbol{K}^{(s)} = H_g^{(s)}\boldsymbol{g} + H_e^{(s)}\boldsymbol{e} \quad (5.12)$$

where

$$K_\xi^{(s)} = \sum_j v_{j\xi}^{(s)}\,(a_j^+ a_j) + \sum_{j\le k} x_{jk\xi}^{(s)}\,(a_j^+ a_j)(a_k^+ a_k) + \ldots \qquad (\xi = \mathrm{g}, \mathrm{e}) \quad (5.13)$$

Such a perturbative Hamiltonian is obtained by keeping in $\boldsymbol{H}^{(s,s)}$ only the $\boldsymbol{g}$ and $\boldsymbol{e}$ components of $\boldsymbol{H}^{(s-1,s)}$ such that $\boldsymbol{m} = \boldsymbol{n}$ and by putting all the other components into $\boldsymbol{R}^{(s-1)}$ to let them be cancelled by the perturbation procedure at order s. Note that the maximum power in the right-hand side of (5.13) increases here as $2s + 2$ compared with $s + 2$ for the procedure for semi-rigid molecules with a single

Fig. 10. Plot of the difference between exact and perturbative quantum energies for the first 91 states of the model Hamiltonian of (5.1) and (5.2) at 10th order of the theory versus energy of each state. The perturbative Hamiltonian, shown in (5.12) and (5.13), consists of two uncoupled Dunham expansions, one for the ground electronic surface and another for the excited surface. The vertical line indicates the energy of the bottom of the excited electronic surface V_e. Notice the sharp increase of the differences above this threshold.

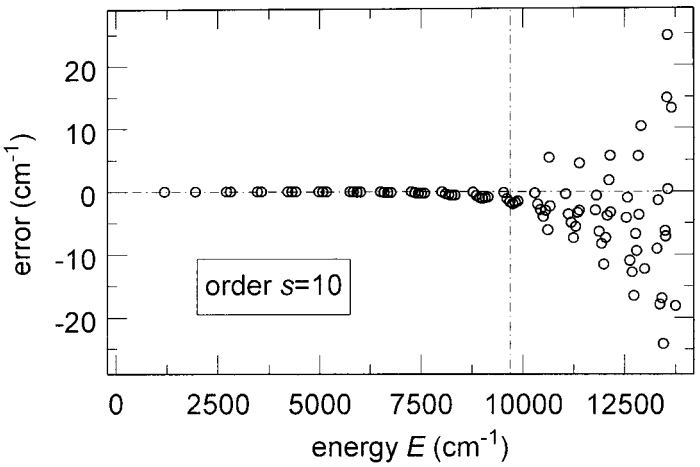

electronic surface cf. (3.8)). The convergence properties of this perturbation series are illustrated in Fig. 9 where the arithmetic average error between the energies of the states of the exact Hamiltonian in (5.1) and (5.2) and those obtained from the perturbative Hamiltonians in (5.12) and (5.13) is plotted as a function of the perturbation order s. Included in the calculations are the first 91 states of the system, whose shifts induced by the diabatic coupling V_c are shown in Fig. 8. Eighty-one states out of these 91 are principally localized in the electronic ground state, while the remaining 10 states are principally localized in the electronic excited state. It can be seen from Fig. 9 that the series converges exponentially up to 10th order but diverges for $s \geq 11$. The average error at order $s = 10$ is as small as 4.1 cm^{-1}, which is particularly impressive when we are reminded that states are shifted by up to 1000 cm^{-1} upon switching on of V_c. The reason for the divergence at order $s = 11$ is easily understood when one looks at Fig. 10, which shows the errors between the energies of exact and perturbative (10th order) quantum states as a function of energy. Indeed, it is seen in this figure that errors remain negligible below the energy of the bottom of V_e, which is indicated by a vertical line, while they increase sharply above this energy. Examination of (5.11) shows that this divergence is most likely due to vibronic resonances, i.e., resonances between states of electronic ground and excited surfaces, which cause some of the $\Sigma_{mn} \mp \delta E$ denominators to become too small and the corresponding terms to diverge.

6. Conclusions

This article has focused on practical solutions for applying CPT to various situations encountered at high vibrational energies (resonances, isomerization, and electronic couplings) and on numerical examples, which demonstrate the efficiency of the proposed procedures. The question as to how the perturbative Hamiltonians obtained are to be handled to extract the physical information encoded therein has deliberately been skipped. The interested reader is referred, for example, to refs. 13–16 for more information on this topic. Before concluding, we would like to mention a few points, which, to our mind, deserve further attention.

First, it should be emphasized that an accurate initial expansion is a sine qua non condition for successful perturbative calculations. For example, it was pointed out in Sect. 3 that convergence of the perturbative series for HCP is limited to the 9th order, because of the poor accuracy of the Taylor expansion at large bending angles (see Fig. 2). Here, this is of little consequence, since the average error

is already as small as 2.4 cm^{-1}. However, it sometimes happens that the Taylor expansion is too poor an approximation to be amenable to perturbative calculations, although this remains an exception rather than the rule. A striking example is the second potential-energy surface for HCP computed by Schinke et al. [75] that is in better agreement with the experimental results than the first one [50,51] discussed in Sect. 3. It turns out that the Taylor expansion computed from this second surface is such a bad approximation that perturbative calculations based thereon are unable to reproduce the energies of all but the lowest quantum states. This is all the more surprising as the dynamics encoded in both spectra are rather similar [13,15,16,50,51,53]. It would, therefore, be interesting to find polynomial expressions that would be more reliable than Taylor expansions for the purpose of subsequent perturbative calculations.

The second remark concerns dissociation, which has not been discussed in this article. Any realistic description of the dissociation dynamics of triatomic molecules necessitates at least two large-amplitude coordinates, namely, the dissociating stretch coordinate and the bend. One can think of a procedure similar to that described in Sect. 4 where both the dissociating stretch (described by exponential functions) and the bend (described by trigonometric functions) would be handled as reactive coordinates. Upon application of the procedure described in Sect. 4, there would then remain only one good quantum number left in the perturbative Hamiltonian that would quantize the inactive coordinate, i.e., the motion along the non-dissociating stretch degree of freedom. Another more complex possibility, which would however result in a larger number of good quantum numbers, would be to use Morse functions to describe the dissociating coordinate, as suggested recently by Child et al. [76]. Everything still has to be done in this domain.

In the end, it is worth mentioning that while all physically "non-important" terms have systematically been dropped from the perturbative Hamiltonian (cf. (2.12)) in this article, one is not obliged to do so. When keeping all terms in the final Hamiltonian — or more precisely all terms up to a maximum order much larger than the perturbation order s — one virtually recovers the exact Hamiltonian [20] provided, of course, that the expansion is accurate enough (see above). The perturbative Hamiltonian, however, has one great advantage compared with the initial one in that the physically non-important terms are strongly reduced by the perturbation procedure. Consequently, the size of the matrices that must be diagonalized to get converged eigenvalues can be substantially smaller for the perturbative Hamiltonian than that for the initial one [20]. To find, with more limited numerical efforts, the exact eigenvalues of systems, which lie today at the limit of usual diagonalization procedures, one can think about applying this technique (i.e., CPT without neglect of physically important terms) to the MEP expansion described in Sect. 4; the mixed Taylor–Fourier expansion is usually more precise and more adaptable to the description of complex surfaces than the Taylor one alone. We plan to test this procedure against the vibrational states of H_2O_2 [77,78] in the near future.

References

1. E.C. Kemble. The fundamental principles of quantum mechanics. McGraw–Hill, New York. 1937.
2. E. Schrödinger. Ann. Phys. (Berlin), **80**, 437 (1926).
3. M.R. Aliev and J.K.G. Watson. *In* Molecular spectroscopy: modern research. Vol. III. *Edited by* K.N. Rao. Academic Press, San Diego. 1985.
4. J.H. Van Vleck. Phys. Rev. **33**, 467 (1929).
5. E.B. Wilson and J.B. Howard. J. Chem. Phys. **4**, 262 (1936).
6. W.H. Shaffer and H.H. Nielsen. Phys. Rev. **56**, 188 (1939).
7. W.H. Shaffer, H.H. Nielsen, and L.H. Thomas. Phys. Rev. **56**, 895 (1939).
8. H.H. Nielsen. Rev. Mod. Phys. **23**, 90 (1951).
9. E.L. Sibert. J. Chem. Phys. **88**, 4378 (1988).
10. X. Wang and E.L. Sibert. J. Chem. Phys. **111**, 4510 (1999).
11. X. Wang, E.L. Sibert, and J.M.L. Martin. J. Chem. Phys. **112**, 1353 (2000).
12. X. Wang and E.L. Sibert. J. Chem. Phys. **113**, 5384 (2000).
13. M. Joyeux, S.Y. Grebenshchikov, and R. Schinke. J. Chem. Phys. **109**, 8342 (1998).

14. D. Sugny, M. Joyeux, and E.L. Sibert. J. Chem. Phys. **113**, 7165 (2000).
15. H. Ishikawa, R.W. Field, S.C. Farantos, M. Joyeux, J. Koput, C. Beck, and R. Schinke. Annu. Rev. Phys. Chem. **50**, 443 (1999).
16. M. Joyeux, S.C. Farantos, and R. Schinke. J. Phys. Chem. A, **106**, 5407 (2002).
17. M. Joyeux. J. Chem. Phys. **109**, 2111 (1998).
18. D. Sugny and M. Joyeux. J. Chem. Phys. **112**, 31 (2000).
19. D. Sugny and M. Joyeux. Chem. Phys. Lett. **337**, 319 (2001).
20. M. Joyeux, D. Sugny, and M. Lombardi. Chem. Phys. Lett. **352**, 99 (2002).
21. G.D. Birkhoff. Dynamical systems. Vol. 9. AMS Colloquium, New York. 1966.
22. F.G. Gustavson. Astron. J. **71**, 670 (1966).
23. R.T. Swimm and J.B. Delos. J. Chem. Phys. **71**, 1706 (1979).
24. T. Uzer, D.W. Noid, and R.A. Marcus. J. Chem. Phys. **79**, 4412 (1983).
25. J.H. Van Vleck. Rev. Mod. Phys. **23**, 213 (1951).
26. I. Shavitt and L.T. Redmon. J. Chem. Phys. **73**, 5711 (1980).
27. D. Papousek and M.R. Aliev. Molecular vibrational-rotational spectra. Elsevier, Amsterdam. 1982.
28. A.B. McCoy and E.L. Sibert. *In* Dynamics of molecules and chemical reactions. *Edited by* R.E. Wyatt and J.Z.H. Zhang. Dekker, New York. 1996.
29. K. Sarka and J. Demaison. *In* Computational molecular spectroscopy. *Edited by* P. Jensen and P.R. Bunker. Wiley, Chichester (England). 2000.
30. K. Nakagawa, S. Tsunekawa, and T. Kojima. J. Mol. Spectrosc. **126**, 329 (1987).
31. J. Tang and K. Takagi. J. Mol. Spectrosc. **161**, 487 (1993).
32. Y.-B. Duan, H.-M. Zhang, and K. Takagi. J. Chem. Phys. **104**, 3914 (1996).
33. Y.-B. Duan and K. Takagi. J. Chem. Phys. **104**, 7395 (1996).
34. Y.-B. Duan, Z.-D. Sun, and K. Takagi. J. Chem. Phys. **105**, 5348 (1996).
35. Y.-B. Duan, L. Wang, and K. Takagi. J. Mol. Spectrosc. **193**, 418 (1999).
36. R. Meyer and H.H. Günthard. J. Chem. Phys. **49**, 1510 (1968).
37. D. Sugny. Ph.D. thesis. Grenoble, France. 2002.
38. E.L. Sibert. J. Chem. Phys. **90**, 2672 (1989).
39. A.B. McCoy and E.L. Sibert. J. Chem. Phys. **92**, 1893 (1990).
40. A.B. McCoy and E.L. Sibert. J. Chem. Phys. **95**, 3476 (1991).
41. A.B. McCoy and E.L. Sibert. J. Chem. Phys. **95**, 3488 (1991).
42. A.B. McCoy, D.C. Burleigh, and E.L. Sibert. J. Chem. Phys. **95**, 7449 (1991).
43. Y. Pak, E.L. Sibert, and R.C. Woods. J. Chem. Phys. **107**, 1717 (1997).
44. C. Jaffé and W.P. Reinhardt. J. Chem. Phys. **71**, 1862 (1979).
45. W.P. Reinhardt. J. Phys. Chem. **86**, 2158 (1982).
46. C. Jaffé and W.P. Reinhardt. J. Chem. Phys. **77**, 5191 (1982).
47. R.B. Shirts and W.P. Reinhardt. J. Chem. Phys. **77**, 5204 (1982).
48. W.P. Reinhardt and D. Farrelly. J. Phys. (Paris), **43**, C2 (1982).
49. K. Sohlberg and R.B. Shirts. J. Chem. Phys. **101**, 7763 (1994).
50. S.C. Farantos, H.-M. Keller, R. Schinke, K. Yamashita, and K. Morokuma. J. Chem. Phys. **104**, 10055 (1996).
51. C. Beck, H.-M. Keller, S.Y. Grebenshchkov, R. Schinke, S.C. Farantos, K. Yamashita, and K. Morokuma. J. Chem. Phys. **107**, 9818 (1997).
52. E.B. Wilson, J.C. Decius, and P.C. Cross. Molecular vibrations. Dover, New York. 1955.
53. M. Joyeux, D. Sugny, V. Tyng, M. Kellman, H. Ishikawa, R.W. Field, C. Beck, and R. Schinke. J. Chem. Phys. **112**, 4162 (2000).
54. J.N. Murrell, S. Carter, and L.O. Halonen. J. Mol. Spectrosc. **93**, 307 (1982).
55. Z. Bacic. J. Chem. Phys. **95**, 3456 (1991).
56. R.A. Marcus. J. Chem. Phys. **45**, 4493 (1966).
57. R.A. Marcus. J. Chem. Phys. **46**, 959 (1967).
58. R.A. Marcus. J. Chem. Phys. **49**, 2610 (1968).
59. W.H. Miller, N.C. Handy, and J.E. Adams. J. Chem. Phys. **72**, 99 (1980).
60. S.K. Gray, W.H. Miller, Y. Yamaguchi, and H.F. Schaefer. J. Chem. Phys. **73**, 2733 (1980).
61. T. Carrington, L.M. Hubbard, H.F. Schaefer, and W.H. Miller. J. Chem. Phys. **80**, 4347 (1984).

62. C. Saint-Espès, X. Chapuisat, and F. Schneider. Chem. Phys. **159**, 377 (1992).
63. X. Chapuisat and C. Saint-Espès. Chem. Phys. **159**, 391 (1992).
64. C. Saint-Espès, X. Chapuisat, and C. Zuhrt. Chem. Phys. **188**, 33 (1994).
65. X. Chapuisat, C. Saint-Espès, C. Zuhrt, and L. Zülicke. Chem. Phys. **217**, 43 (1997).
66. F. Gatti, Y. Justum, M. Menou, A. Nauts, and X. Chapuisat. J. Mol. Spectrosc. **181**, 403 (1997).
67. M. Joyeux, D. Sugny, M. Lombardi, R. Jost, R. Schinke, S. Skokov, and J. Bowman. J. Chem. Phys. **113**, 9610 (2000).
68. R. Jost, M. Joyeux, and M. Jacon. Chem. Phys. **283**, 17 (2002).
69. H. Köppel, W. Domcke, and L.S. Cederbaum. Adv. Chem. Phys. **57**, 59 (1984).
70. W. Domcke and G. Stock. Adv. Chem. Phys. **100**, 1 (1997).
71. I.B. Bersucker and V.Z. Polinger. Vibronic interactions in molecules and crystals. Springer, Berlin. 1989.
72. G. Herzberg and H.C. Longuet-Higgins. Discuss. Faraday Soc. **35**, 77 (1963).
73. T. Carrington. Discuss. Faraday Soc. **53**, 27 (1972).
74. D.R. Yarkony. Rev. Mod. Phys. **68**, 985 (1996).
75. C. Beck, R. Schinke, and J. Koput. J. Chem. Phys. **112**, 8446 (2000).
76. M.S. Child, M.P. Jacobson, and C.D. Cooper. J. Phys. Chem. A, **105**, 10791 (2001).
77. B. Kuhn, T. Rizzo, D. Luckhaus, M. Quack, and M.A. Suhm. J. Chem. Phys. **111**, 2565 (1999).
78. R. Chen, G. Ma, and H. Guo. Chem. Phys. Lett. **320**, 567 (2000).